Investigation of AC Copper and Iron Losses in High-Speed High-Power Density PMSM

Ahmed Al-Timimy, Paolo Giangrande, Michele Degano, Michael Galea and Chris Gerada

***Abstract* – This paper presents a detailed investigation of AC copper losses in high-speed high-power density permanent magnet synchronous machine. For parallel strands winding, it is not easy to accurately estimate the AC copper losses using finite element model (FEM), due to the random distribution of the conductors inside the slots. Therefore, this work is focused on the separation of the AC copper losses component from the total measured losses. In order to obtain more precise results, the effect of manufacturing process on the stator core has also been considered. A 3D FEM has been used to evaluate the total power losses including the effect of the end-windings. Finally, the influence of the temperature on the AC losses is taken into account by monitoring the winding temperature during the experiments.**

***Index Terms* -- AC copper losses, end-windings, manufacturing processes, permanent magnet motors, skin and proximity effects.**

I. Introduction

FOR high-speed and high-power density applications, where the machine needs to achieve high efficiency over all the operating range, an accurate prediction of power losses distribution is very important [1]. One of the major power losses contribution, for the permanent magnet synchronous machines (PMSMs), is given by the stator winding losses [2-3]. For high-speed applications, the electrical resistance of the winding increases with the operational speed due to two different phenomena, namely skin and proximity effects; thus leading to additional AC losses [4-5]. Therefore, the contribution of the AC copper losses to the overall losses must be identified accurately to estimate the machine performance. The AC copper losses have been widely investigated in literature [1-10]. While, less attention was paid to the segregation of the AC copper losses from the total measured losses considering the effect of manufacturing process on the stator core. The machining of the stator core affects the magnetic material properties. Indeed, the specific core losses increase and inaccuracies are introduced when the AC copper losses are segregated from the total measured power [10-12]. In particular, this effect becomes more significant during high frequency operations. The aim of this work consists in identifying the AC copper losses at different operating frequencies and temperatures, by considering the impact of manufacturing process on the stator core. To reach the aim, a complete wound stator has been used during the experimental study for achieving a more accurate representative of the electromagnetic field distribution. In addition, the end-winding influence, the stator core manufacturing process effect and thermal behavior are included in the proposed investigation.

The machine prototype together with the details of the high-speed application are presented in section II. Section III describes the AC copper losses generated in a PMSM. The FEM of the assembled stator core winding is introduced in section IV. While, the experimental setup and the adopted test procedure are highlighted in section V. The experimental characterisations of the magnetic material properties for the stator core are analysed. Their influence on the AC copper losses and phase resistance at different operating conditions are provided in section VI. Finally, section VII draws practical and useful considerations to take into account when designing high-speed machines.

II. PM Machine Prototype

In this work a high-speed high-power density, 8 poles / 9 slots, PMSM prototype, optimized for a direct coupled pump application, is considered as a study case. The details of the electromagnetic design, optimization and thermal management are not included in this paper, as these are covered in other author's publications [13-16]. For sake of clarity, the 8 poles / 9 slots PMSM cross-sectional area is shown in Fig. 1. A cobalt iron (CoFe) material (Vacoflux 48), with lamination thickness of 0.1 mm and saturation limit of 2.3 T has been chosen for the stator core [14].

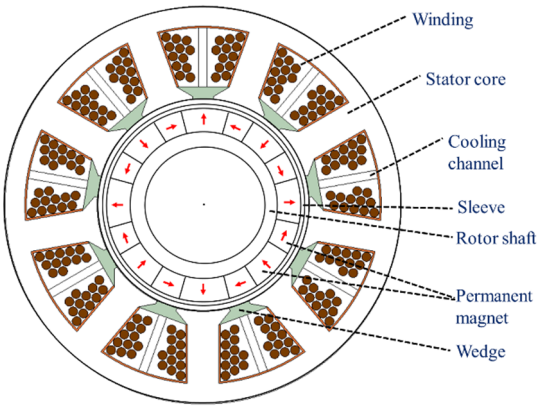

Fig. 1. Cross-section of the 8 poles / 9 slots PMSM machine.

The stator core and the windings are cooled via a cooling channels inside the slot in order to achieve a higher power to mass ratio [17-18]. A copper fill factor of 37% of the slot area represents a reasonable compromise between the cooling channel area and the generated copper losses. In addition, multi-strands parallel conductor arrangement has been used in order to reduce the AC copper losses. The

Ahmed Al-Timimy, Paolo Giangrande, Michele Degano, Michael Galea and Chris Gerada are with the Power Electronics, Machines and Control Group, The University of Nottingham, University Park, Nottingham, NG7 2RD, UK.

Michele Degano, Michael Galea and Chris Gerada are also with the Power Electronics, Machines and Control Group, University of Nottingham Ningbo China, Ningbo, China.

Ahmed Al-Timimy (e-mail: Ahmed.Al-Timimy@nottingham.ac.uk)

permanent magnets are mounted on the rotor surface in a quasi-Halbach configuration. The retention is given by a titanium sleeve holding the magnets on a hollow shaft made of permeable 17-4PH stainless steel [19-20]. Table I lists the main design parameters of the PMSM prototype.

TABLE I
MAIN DESIGN PARAMETERS OF THE INVESTIGATED MACHINE

Parameter	Value
Maximum speed	19 krpm
DC Link voltage	270 Vdc
Maximum phase current	85 A
Stack Length	80 mm
Stator outer diameter	70 mm
Split ratio	0.535
Current density	27.2 (A/mm^2)

III. COPPER LOSSES IN PMSM

In general, for the high-power density applications using an appropriate cooling system, the electrical loading is increased to achieve the required output power. However, the resulting copper losses lead to a temperature rise in the windings, which might reduce the insulation lifetime as well as reaching the thermal limit of the machine [21-22]. Fig. 2 shows the percentage of losses calculated in different parts of the PMSM at maximum speed (i.e. worst-case scenario). For this application, the copper losses represent the 54% of the machine total losses. Therefore, it is necessary to calculate the total copper losses (AC+DC) to have an accurate estimation of the machine performance.

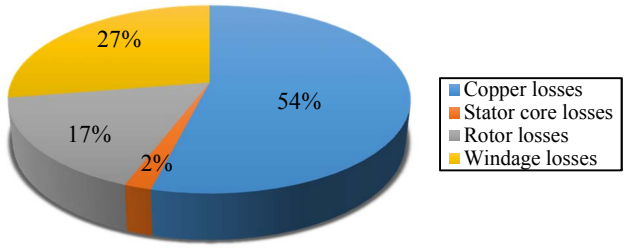

Fig. 2. Break-down of the losses at maximum speed.

In PMSM, the increased copper losses with the frequency is mainly due to the skin and proximity effects, which influence the winding resistance value. Both phenomena are caused by eddy currents. In the first case (i.e. skin effect), the eddy currents are self-induced, while in the second case (i.e. proximity effect), they are due to either 1) the current flowing through close by conductors or 2) the magnetic field produced by the moving permanent magnets [7, 9]. The self-induced eddy currents cause a non-uniform current density distribution within the conductor due to AC current passing through the conductor itself. The skin effect depends on the frequency and the dimensions of the conductor and it can be dealt by choosing a conductor with diameter smaller than the skin depth δ [7], which is given by (1).

$$\delta = \sqrt{\frac{\rho}{\pi f \mu_o \mu_r}} \quad (1)$$

Where, ρ and μ_r are the electrical resistivity and the relative permeability of the conductor, respectively, f and μ_o are the frequency and the permeability of the free space, respectively. The proximity effect is dependent on how the conductors are placed inside the slots and it can be mitigated by using either windings with parallel strands (resulting in smaller diameter of the conductor) or Litz wires (thinner wire strands connected in parallel) [7-8]. The main disadvantages rising from the adoption of windings with parallel strands are represented by the higher manufacturing complexity and the unbalanced current distribution across the strands. The latter results in a circulating current effect [9]. On the other hand, by using windings with parallel stands, a greater fill factor could be achieve with lower cost with respect to the Litz wire. Therefore, the DC resistance of the phase winding must be computed including a factor that takes into account the AC losses due to the induced eddy currents.

IV. FE MODELLING

Both 2D and 3D FEMs have been implemented to accurately simulate the AC copper losses of the designed PMSM (i.e. fractional slot machine with non-overlapped concentrated winding). Fig. 3 depicts the 3D FEM, where each solid conductor has been modelled and connected via an external circuit. This modelling approach allows to identify the skin and proximity effects in both active-length and end-winding regions.

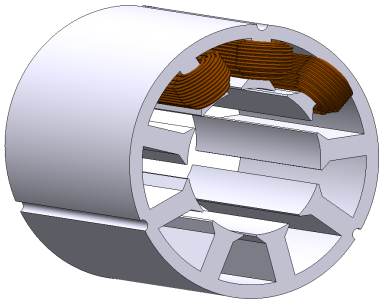

Fig. 3. 3D FEM including both active-length and end-winding regions.

In order to reduce the simulation time of the 3D FEM, a model with only to one phase winding has been considered. In addition, a refined mesh for the copper wire strands has been set for a precise distribution of the currents at high frequency [4]. The phase winding consists in 3 series connected coils, which are made of 12 turns each. Further, the turns are arranged on 4 strands per turn and a 0.873 mm diameter wire (including the insulation thickness) is adopted for the strand. Every coil has been modelled by means of a specific circuit within the FE software.

V. EXPERIMENTAL SETUP

The experimental tests have been carried out on a complete wound stator, as illustrated in Fig. 4, while, Fig. 5 shows the setup used to measure the winding losses. A variable-frequency power supply with sinusoidal current (Chroma 61511) is employed to energize the winding. Power, voltage and current are measured using a high bandwidth power analyzer (KinetiQ PPA2530), which allows to take into account the resistance variation with frequency. K-type thermocouples, placed within the end-winding and the middle section of the winding (i.e. on the winding active-length), are used for monitoring the temperature. For

the experimental measurements, the winding losses are obtained as the difference between the total input power measured through the power analyzer and the core losses estimated by the 3D FEM. In terms of core losses estimation, more precise results are achieved by performing the material characterization of the stator core. Indeed, the actual specific core losses (including the manufacturing process effect) is experimentally determined. The material characterization represents an important step, since the manufacturing process strongly influences the estimated ratio between AC and DC copper losses, as discussed in the next section. The winding temperatures are recorded at several excitation currents and frequencies. The thermal test for a single excitation point is performed until the thermal steady state is reached [2]. Hence, the thermal test is stopped once the winding temperature varies with a ratio slower than 1°C over 10 minutes. In Fig. 6, the measured temperatures are reported for an applied current of 25 Arms is applied at several frequencies.

Fig. 4. Tested stator core and winding arrangement.

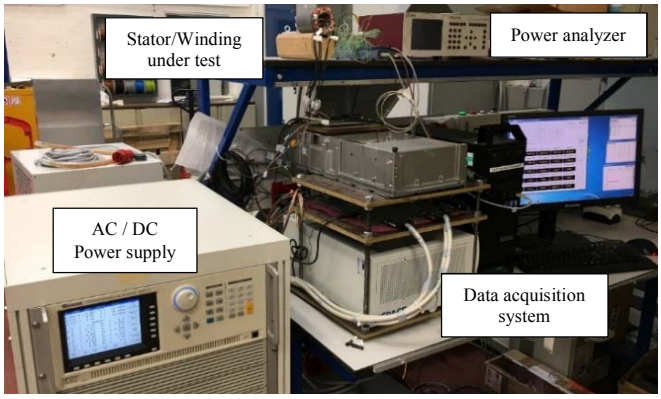

Fig. 5. Experimental setup.

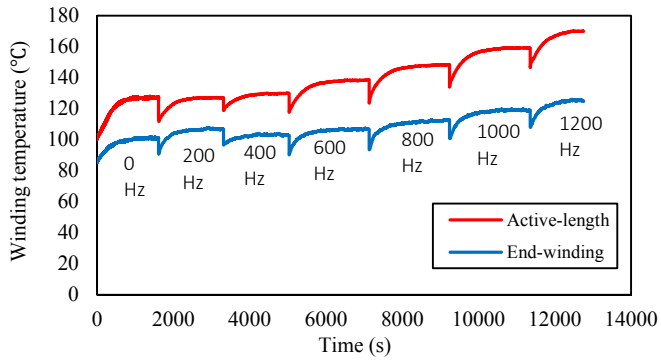

Fig. 6. Winding temperature under $I_{rms} = 25\ A$ with different frequencies.

A significant difference between the temperature inside the slot (i.e. active-length winding) and the one measured in the end-winding is recorded. The temperature mismatch is caused by the different heat path crossed. In fact, the heat generated within the end-windings is easily released to the ambient, since they are directly exposed to the air (i.e. the stator core under test is not equipped with housing). Conversely, the heat produced by the active-length winding should cross the stator back iron before being dissipated to the ambient. Therefore, the temperature inside the slot represents the hot-spot of the stator core under study.

VI. AC Losses Analysis

A. *Stator core losses*

It is not possible to experimentally segregate the laminated stator core losses from the meaused power (i.e. copper losses + iron losses) using the power analyser [1, 2]. Therefore, accurate estimation of iron losses is required. For this purpose, FE simulations of the stator core are performed adopting the same current and frequency values used during the experiments. Since the stator core is manufactured by means of several machining processes, its magnetic properties, such as magnetization BH curve and the specific core losses, will change. For this reason, it is necessary to quantify these changes in the magnetic properties to accurately determine the AC copper losses term. As previously mentioned, the stator core is made of CoFe material, which approximately consists of 49% cobalt, 49% iron and 2% vanadium [23-24]. Table II gives an overview of the CoFe material properties provided by the manufacturer's datasheet.

TABLE II
Material Properties of the Investigated CoFe Stator Core

Lamination Thickness	Density	Electrical Resistivity	Package Density	Saturation Flux Density
0.1 mm	8120 kg/m^3	0.4 µohm	98%	2.3 T

Fig. 7. Investigated stator core with and without measured coils.

A state of art testing facility that is available in-house is employed to characterize the stator core shown in Fig. 7 [25-26]. The core losses tests are performed under pure sine wave excitation. The obtained specific core losses, as a function of different frequencies (up to 2 kHz) and flux densities (from 1 to 2 T), are reported in Fig. 8. Considering the results of Fig. 8, the specific core losses increases as the flux density and the frequency rise. Comparing the experimental data against the ones given by the

manufacturer's datasheet, higher specific core losses are measured due to the manufacturing process [25]. According to the material characterization outcomes, the material database in the FE software has been updated considering the measured specific core losses. The iron losses computed using the specific core losses provided by the manufacturer's datasheet are presented in Fig. 9 (a), where the results obtained from both 2D and 3D FEMs are compared (the 3D FEM models also the end-windings).

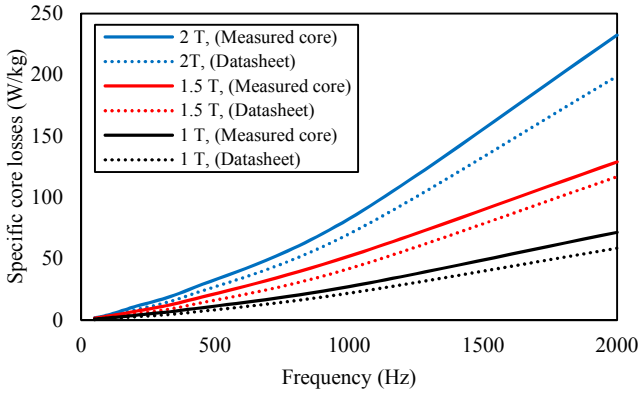

Fig. 8. Comparison between specific core losses as function of both frequency and flux density.

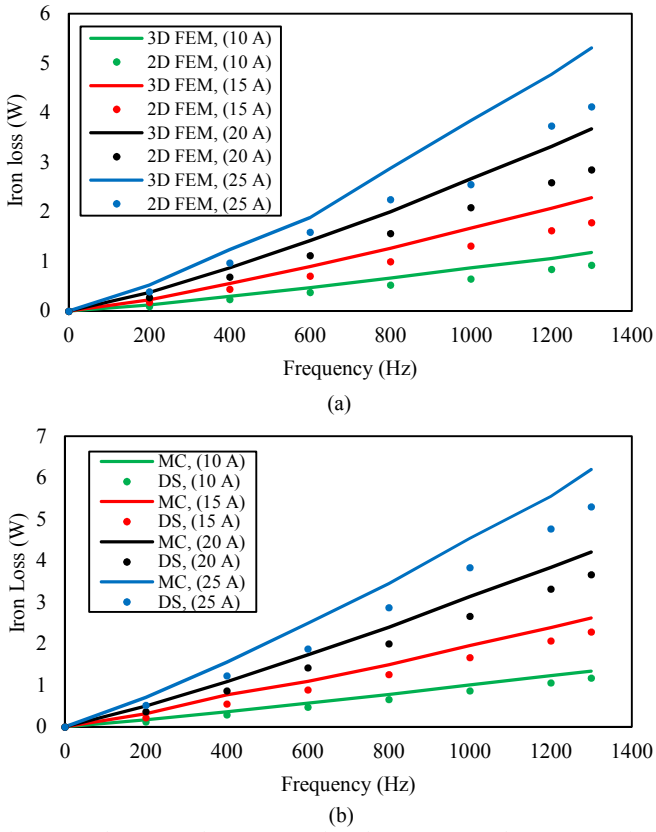

Fig. 9. Iron losses trends: (a) comparison between 2D and 3D FEMs using the manufacturer data and (b) comparison between the measured and datasheet data using the 3D FEM.

Due to the end effect [26], the core losses resulting from the 3D FEM are higher than the ones provided by the 2D FEM. Indeed, the end-winding leakage flux causes a local flux density increment in the edge of tooth-shoe region, as highlighted in Fig. 10 (a), which leads to extra core losses. In Fig. 9 (b), the core losses obtained using the manufacturer's datasheet data (DS) are compared against the ones determined using the material characterization data (MC). Fig. 10 (b) shows the distribution of the magnetic flux density in the stator conductors. The stator slot leakage flux is higher in the slot opening region compared to the slot top region. Therefore, the largest eddy currents are induced close to the slot opening [27].

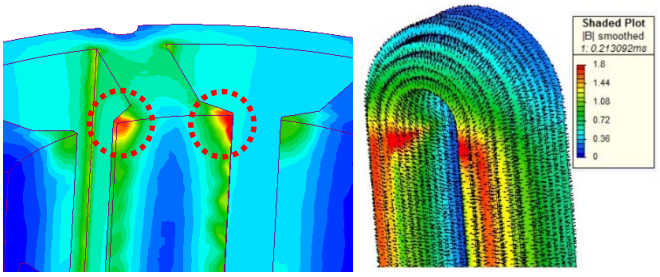

(a) (b)

Fig. 10. 3D FEM flux density distributions: (a) in the stator core and (b) in the winding (active length and end-winding).

B. *AC copper losses*

The total winding power is sum of two terms, namely the losses in the active-length $P_{act}(T,f)$ and the losses in the end-winding $P_{end}(T,f)$, as expressed by (2).

$$P_{tot}(T,f) = P_{act}(T,f) + P_{end}(T,f) \quad (2)$$

Both losses terms are function of the temperature (T) and the frequency (f). During DC operations, the two losses terms can be easily identified knowing the DC winding resistance and total length of winding (active + end-winding lengths). For this analysis, the electrical resistivity of the copper can be corrected according to (3), where, ρ_o is the electrical resistivity of copper at $T_o = 20°C$ ($\rho_o = 1.68 \cdot 10^{-8}\ \Omega m$), α is the temperature coefficient of resistivity ($\alpha = 0.00393$) and T is the operating point temperature.

$$\rho = \rho_o * (1 + \alpha(T - T_o)) \quad (3)$$

In case of AC operations, (3) cannot be directly used to correct the operating temperature. Since, the DC and AC copper losses terms are depending on the temperature in different manner [1].

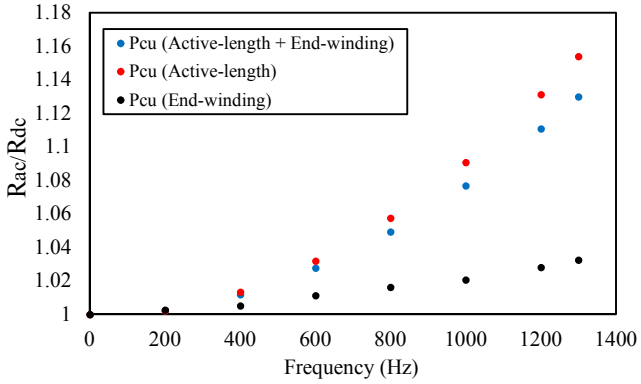

Fig. 11. AC winding losses factor ($R_{ac}/R_{dc}\,|_T$) at $I_{rms} = 25\ A$ and 20°C.

Based on [28], the temperature dependency of the AC copper losses ($P_{ac}|_T$) is expressed by (4).

$$P_{ac}|_T = P_{dc}|_{T_O}\big(1+\alpha(T-T_o)\big) + P_{dc}|_{T_O}\frac{\frac{R_{ac}}{R_{dc}}|_{T-1}}{(1+\alpha(T-T_o))^{\beta}} \quad (4)$$

where, $P_{dc}|_{T_O}$ are the DC copper losses at T_o (i.e $P_{dc}|_{T_O} = 3I^2_{rms}R_{dc}|_{T_O}$), β is a correction factor (value between 0 and 1), which is determined by curve fitting (4) into the AC copper losses data at the temperature T. Finally, $R_{ac}/R_{dc}|_T$ is the AC winding losses factor defined as the ratio between AC to DC resistances [28-29]. The trend of the AC winding losses factor ($R_{ac}/R_{dc}|_T$) as function of the frequency is presented in Fig. 11. For the end-winding, the R_{ac}/R_{dc} ratio is very small compared to the one of the active-length winding. This is due to fact that the leakage flux along the active-length winding is higher than in the end-winding region, where the windings are surrounded by air [4, 30]. Therefore, lower proximity losses occur in the end-winding area.

C. *Experiment results and analysis*

In the previous section, the AC to DC resistance ratio has been evaluated using 3D FEM. However, for random-wound windings, the uncertainty in the conductors' distribution within the slot affects the AC copper losses estimation since it is difficult to exactly simulate the actual conductors' distribution. Therefore, the stator core input power has been measured using a power analyzer and the FE iron losses have been subtracted from the measured power to accurately determine the AC copper losses. Fig. 12 (a) shows the copper losses at several frequencies obtained using the 3D FEM, which includes the temperature dependency of the resistivity.

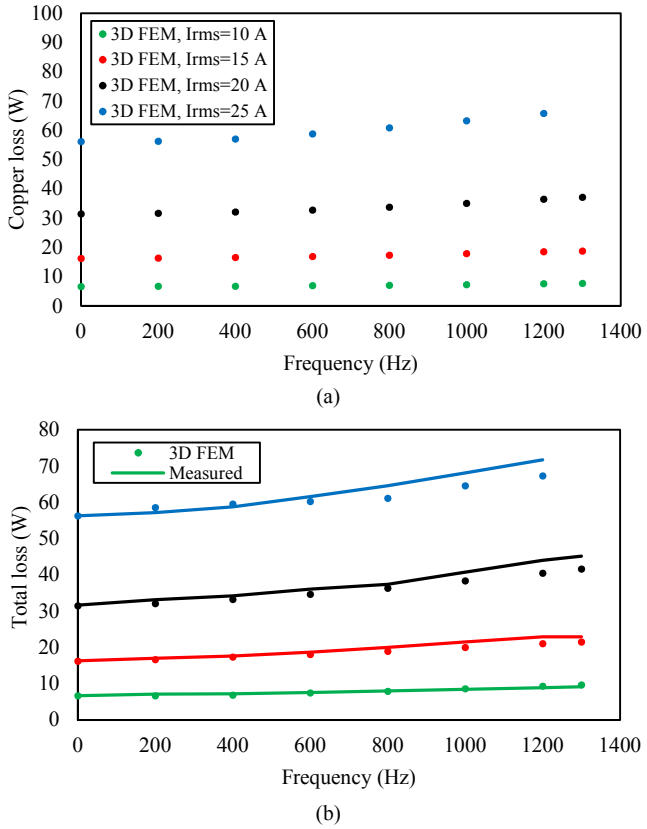

Fig. 12. Variation of the losses with the frequency: (a) copper losses and (b) total losses.

Fig. 12 (b) reports the comparison between measured and calculated total power losses. The latter are determined as sum between the copper losses of Fig. 12 (a) and the iron losses of Fig. 9 (b). The results are in good agreement and the slightly mismatch is due to the random distribution of the conductors. Indeed, parallel strands with random placement have a significant impact on the AC copper losses due to the increase in the circulating current over frequency. To investigate the influence of the core losses segregation on the measured phase resistance, a sensitivity analysis has been carried out. In order to obtain the DC and AC phase resistances (R_{dc} and R_{ac}), the input power per phase and the rms current have been measured using the power analyzer. Further, the winding temperatures have been recorded during the experimental tests. The AC phase resistance has been determined over a wide range of frequency (from 150 Hz to 1300 Hz). In Fig. 13 (a), the link between the DC phase resistance and the winding temperature is highlighted, whereas the dependency of the AC phase resistance with the frequency is outlined in Fig. 13 (b). Looking at Fig. 13 (b), the AC phase resistance value increases with the frequency, as expected.

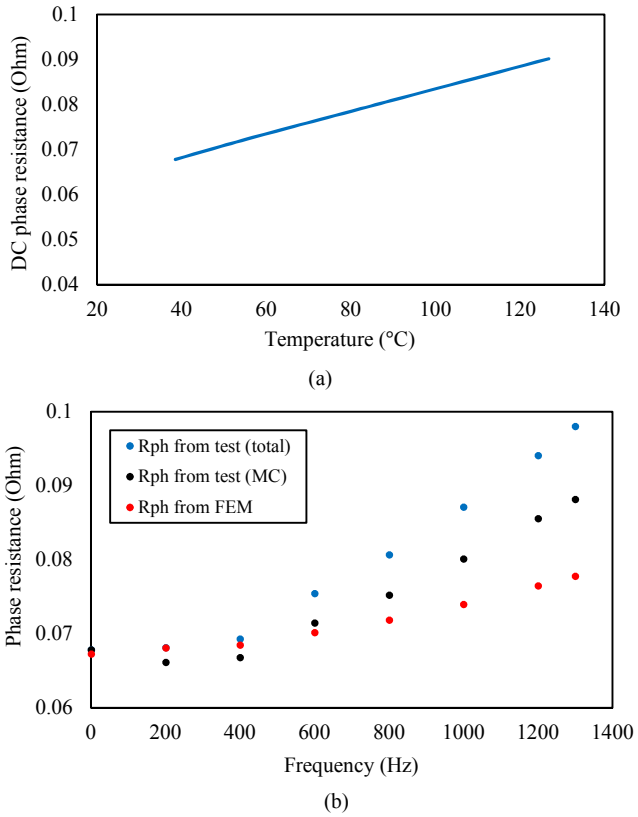

Fig. 13. Phase resistance trends: (a) DC resistance versus temperature and (b) AC resistance versus. frequency at $I_{rms} = 10\ rms$.

To accurately determine the AC phase resistance, the iron losses $P_{fe\_(MC)}$ (calculated through 3D FE simulations) are subtracted from the total measured power P_{in}, as shown in (5).

$$R_{ph\_ac} = \frac{P_{in} - P_{fe\_(MC)}}{I^2_{rms}} \quad (5)$$

It is important to underline that the measured specific core

losses, obtained by means of the material characterization, are adopted during the 3D FE simulations performed for quantifying the iron losses ($P_{fe\_(MC)}$). Using the material characterization data of the stator core, more accurate results are achieved, as shown in Fig. 13 (b). The measured value of $R_{ph\_ac\_MC}$ at 1200 Hz is 9.08% lower compared to the total measured phase resistance R_{ph_ac}. While, an 11.86% difference is found between $R_{ph\_ac\_MC}$ and $R_{ph\_ac\_FEM}$ at 1200 Hz. This is due to fact that the parallel strands are placed randomly in the slot and therefore more AC losses are generated at higher frequencies. In fact, moving towards lower operating frequencies, the mismatch between $R_{ph\_ac\_MC}$ and $R_{ph\_ac\_FEM}$ values is smaller.

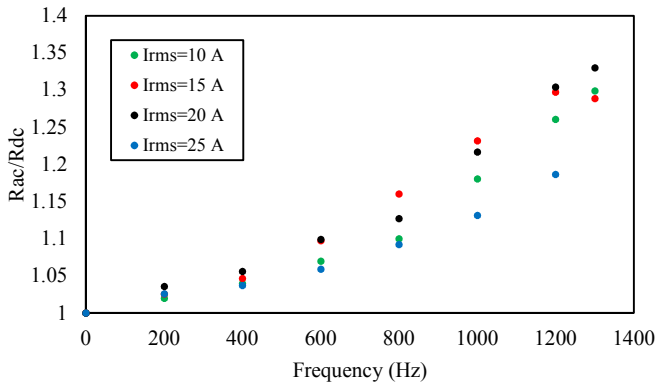

Fig. 14. Measured R_{ac}/R_{dc} ratio versus frequency at winding operating temperature.

Fig. 14 shows the R_{ac}/R_{dc} ratio versus the frequency at the winding operating temperature. It's observed that the rate of increase in the AC losses component drops with the increased temperature and the current level. This trend is explained by the higher copper electrical resistivity with the winding temperature increment, which leads greater DC copper losses. Hence, a lower the R_{ac}/R_{dc} ratio is revealed [1, 5]. Further, with higher current level, the rate of increase of the DC copper losses is higher with respect to AC losses component, since the power is proportional to current squared.

VII. Conclusion

In this paper, the AC copper losses of a high-speed high-power density PMSM have been investigated and discussed. The influence of the variations in the stator core material properties (due to manufacturing processes) have been taken into account during the investigation. A complete stator / winding assembly motor has been used for both FE simulations and measurements to have more detailed representative of the electromagnetic conditions occurring in the full machine. The analysis has been carried out though 2D and 3D FEMs, where the latter includes the effect of end-winding. The obtained results have been compared with the experimental data.

In general, it's found that for the machines with parallel strands copper winding, the experimental approach provides more accurate results than FE simulation regarding to the AC copper losses estimation. This is due by the random arrangement of the conductors inside the slot of the manufactured machine, which has a significant effect on the AC copper losses. Also, it's found that AC copper losses generated within the end-winding are very small.

The segregation of the AC copper losses component from the total measured losses can be greatly influenced by the stator core losses estimated in 3D FEM. To reflect the variation in the material properties due to the manufacturing process, the stator core has been experimentally characterized. It is shown that the iron losses determined by using the measured specific core losses (at 1200 Hz and 25 A) are 13.2% higher than the ones calculated by means of the specific core losses value provided by the manufacturer's datasheet. This difference in iron losses leads to 9.08% difference in the measured phase resistance (at 1200 Hz and 25 A). The phase resistance mismatch is subject to further increment as both the operating current and frequency increase.

Finally, the presented study confirmed that the effects of manufacturing processes on the stator core can influence the separation of the AC copper losses from the total measured losses. Hence, such effects are required to be accounted for the accurate estimation of phase resistance. In particular, for higher performance and higher speed applications, the above aspect needs to be considered for an accurate estimation of the overall machine performance.

VIII. Acknowledgment

This work is supported in part by the Higher Committee for Education Development (HCED) in Iraq.

IX. References

[1] R. Wrobel, A. Mlot and P. H. Mellor, "Contribution of End-Winding Proximity Losses to Temperature Variation in Electromagnetic Devices," in *IEEE Transactions on Industrial Electronics*, vol. 59, no. 2, pp. 848-857, Feb. 2012.

[2] A. Mlot, M. Lukaniszyn and M. Korkosz, "Influence of an end-winding size on proximity losses in a high-speed PM synchronous motor," *2015 Selected Problems of Electrical Engineering and Electronics (WZEE)*, Kielce, 2015, pp. 1-6.

[3] C. Sciascera, P. Giangrande, C. Brunson, M. Galea and C. Gerada, "Optimal design of an electro-mechanical actuator for aerospace application" in *41st Annual Conference of the IEEE Industrial Electronics Society* (IECON 2015), pp. 1903-1908, November 2015.

[4] D. A. Gonzalez and D. M. Saban, "Study of the Copper Losses in a High-Speed Permanent-Magnet Machine With Form-Wound Windings," in *IEEE Transactions on Industrial Electronics*, vol. 61, no. 6, pp. 3038-3045, June 2014.

[5] D. Bauer, P. Mamuschkin, H. C. Reuss and E. Nolle, "Influence of parallel wire placement on the AC copper losses in electrical machines," *2015 IEEE International Electric Machines & Drives Conference (IEMDC)*, Coeur d'Alene, ID, 2015, pp. 1247-1253.

[6] P.Giangrande, C.I.Hill, S.V.Bozhko, and C. Gerada, "A novel multi-level electro-mechanical actuator virtual testing and analysis tool", *in 7th IET Conference on Power Electronics, Machines and Drives* (PEMD), pp. 1-6, 2014.

[7] F. Jiancheng, L. Xiquan, B. Han and K. Wang, "Analysis of Circulating Current Loss for High-Speed Permanent Magnet Motor," in *IEEE Transactions on Magnetics*, vol. 51, no. 1, pp. 1-13, Jan. 2015.

[8] S. Iwasaki, R.P. Deodhar, Y. Liu, A. Pride, Z.Q. Zhu and J.J. Bremner, "Influence of PWM on the Proximity Loss in Permanent-Magnet Brushless AC Machines," in *IEEE Transactions on Industry Applications*, vol. 45, no. 4, pp. 1359-1367, July-aug. 2009.

[9] M. van der Geest, H. Polinder, J. A. Ferreira and D. Zeilstra, "Stator winding proximity loss reduction techniques in high speed electrical machines," *2013 International Electric Machines & Drives Conference*, Chicago, IL, 2013, pp. 340-346.

[10] P. Mellor, R. Wrobel, D. Salt and A. Griffo, "Experimental and analytical determination of proximity losses in a high-speed PM machine," *2013 IEEE Energy Conversion Congress and Exposition*, Denver, CO, 2013, pp. 3504-3511.
[11] S.A. Odhano, P. Giangrande, R. Bojoi and C. Gerada, "Self-commissioning of interior permanent magnet synchronous motor drives with high-frequency current injection," in *5th IEEE Energy Conversion Congress and Exposition (ECCE),* Denver, Colorado, USA, 2013, pp. 3852-3859.
[12] S.A. Odhano, P. Giangrande, I.R. Bojoi, and C. Gerada, "Self-commissioning of interior permanent magnet synchronous motor drives with high-frequency current injection", in *IEEE Transactions on Industry Applications*, vol. 50, n. 5, pp. 3295-3303, September 2014.
[13] A. Al-Timimy, M. Degano, P. Giangrande, G. Lo Calzo, Z. Xu, M. Galea, C. Gerada, H. Zhang, and L. Xia, "Design and optimization of a high power density machine for flooded industrial pump," in *2016 XXII International Conference on Electrical Machines (ICEM)*, Lausanne, 2016, pp. 1480-1486.
[14] A. Al-Timimy, M. Degano, Z. Xu, G. Lo Calzo, P. Giangrande, M. Galea, C. Gerada, H. Zhang, and L. Xia, "Trade-off analysis and design of a high power density PM machine for flooded industrial pump," in *42nd Annual Conference of the IEEE Industrial Electronics Society* (IECON), Florence, 2016, pp. 1749-1754.
[15] Z. Xu, A. Al-Timimy, M. Degano, P. Giangrande, G. Lo Calzo, H. Zhang, M. Galea, C. Gerada, S. Pickering, L. Xia, "Thermal management of a permanent magnet motor for a directly coupled pump," in *XXII International Conference on Electrical Machines (ICEM)*, Lausanne, 2016, pp. 2738-2744.
[16] A. Al-Timimy, P. Giangrande, M. Degano, Z. Xu, M. Galea, C. Gerada, G. Lo Calzo , H. Zhang, and L. Xia, "Design and Losses Analysis of a High Power Density Machine for Flooded Pump Applications" in press on *IEEE Transaction on Industrial Applications*, 2018, DOI: 10.1109/TIA.2018.2821623.
[17] V. Madonna, P. Giangrande, and M. Galea, "Electric Power Generation in Aircraft: review, challenges and opportunities," in press on *IEEE Transaction on Transportation Electrification*, 2018, DOI 10.1109/TTE.2018.2834142.
[18] C. I. Hill, S. Bozhko, Y. Tao, P. Giangrade, and C. Gerada, "More Electric Aircraft Electro-Mechanical Actuator Regenerated Power Management," in *24th International Symposium on Industrial Electronics* (ISIE), pp. 337-342, 2015.
[19] A. Al-Timimy, M. Alani, M. Degano, P. Giangrande, C. Gerada and M. Galea, "Influence of Rotor Endcaps on the Electromagnetic Performance of High Speed PM Machine" in press on *IET Electric Power Applications*, 2018, DOI: 10.1049/iet-epa.2017.0811.
[20] A. Al-Timimy, P. Giangrande, M. Degano, M. Galea, and C. Gerada, "Comparative study of permanent magnet-synchronous and permanent magnet-flux switching machines for high torque to inertia applications," in *2017 IEEE Workshop on Electrical Machines Design, Control and Diagnosis* (WEMDCD), pp. 45-51, 2017.
[21] C. Sciascera, P. Giangrande, L. Papini, C. Gerada and M. Galea, "Analytical Thermal Model for Fast Stator Winding Temperature Prediction", *IEEE Transactions on Industrial Electronics,* vol. 64, n. 8, pp. 6116-6126, 2017.
[22] C. Sciascera, M. Galea, P. Giangrande, and C. Gerada, "Lifetime consumption and degradation analysis of the winding insulation of electrical machines," in *IET Internatoional Conference on Power Electronics Machines and Drives* (PEMD), pp. 1-6, 2016.
[23] A. Krings, A. Boglietti, A. Cavagnino and S. Sprague, "Soft Magnetic Material Status and Trends in Electric Machines," in *IEEE Transactions on Industrial Electronics*, vol. 64, no. 3, pp. 2405-2414, March 2017.
[24] Volbers, Niklas, and Joachim Gerster. "High saturation high strength iron-cobalt alloy for electrical machines." Proceedings of the INDUCTICA, CWIEME Berlin (2012).
[25] A. Al-Timimy, G. Vakil, M. Degano, P. Giangrande, C. Gerada and M. Galea, "Considerations on the Effects that Core Material Machining has on an Electrical Machine's Performance," in press on *IEEE Transactions on Energy Conversion*, vol. PP, no. 99, pp. 1-1. DOI: 10.1109/TEC.2018.2808041.
[26] F. Cupertino, G. Pellegrino, P. Giangrande and L. Salvatore, "Model based design of a sensorless control scheme for permanent magnet motors using signal injection," in *Energy Conversion Congress and Exposition (ECCE),* Atlanta, USA, September 2010, pp. 3139-3146.
[27] T. Noguchi and T. Komori, "Eddy-current loss analysis of copper-bar windings of ultra-high-speed PM motor," *2015 International Conference on Electrical Systems for Aircraft, Railway, Ship Propulsion and Road Vehicles (ESARS)*, Aachen, 2015, pp. 1-6.
[28] R. Wrobel, D. E. Salt, A. Griffo, N. Simpson and P. H. Mellor, "Derivation and Scaling of AC Copper Loss in Thermal Modeling of Electrical Machines," in *IEEE Transactions on Industrial Electronics*, vol. 61, no. 8, pp. 4412-4420, Aug. 2014.
[29] A. Fatemi, D. M. Ionel, N. A. O. Demerdash, D. A. Staton, R. Wrobel and Y. C. Chong, "A computationally efficient method for calculation of strand eddy current losses in electric machines," in *Energy Conversion Congress and Exposition (ECCE)*, 2016, pp. 1-8.
[30] P. Giangrande, F. Cupertino and G. Pellegrino, "Modelling of linear motor end-effects for saliency based sensorless control," in *Energy Conversion Congress and Exposition (ECCE),* Atlanta, USA, September 2010, pp. 3261-3268.

X. BIOGRAPHIES

Ahmed Al-Timimy received his M.Sc. degree in Electrical Engineering from the University of Technology, Baghdad, Iraq in 2012. He is currently working towards his PhD in electro-magnetic modelling and electrical machine design within the Power Electronics, Machines and Control (PEMC) Group at The University of Nottingham, Nottingham, UK. His main research interests are design and analysis of high performance electrical machines for aerospace applications.

Paolo Giangrande received the Bachelor's (Hons.) and Master's (Hons.) degrees in electrical engineering at the Politecnico of Bari in 2005 and 2008, respectively. During 2008, he was a Marie Curie Intra-European Fellow at the University of Malta. He received his PhD in electrical engineering at the Politecnico of Bari in 2011. Since January 2012, he is Research Fellow at the University of Nottingham (UK), within the Power Electronics, Machines and Control Group. From 2017, he is the head of the Accelerated Lifetime Testing Laboratory at the Institute of Aerospace Technology, Nottingham. His main research interests include sensorless control of AC electric drives, design and testing of electromechanical actuators for aerospace, thermal management of high-performance electric drives and reliability and lifetime modelling of electrical machines.

Michele Degano (M'15) received the Laurea degree in electrical engineering from the University of Trieste, Trieste, Italy, in 2011, and the Ph.D. degree in industrial engineering from the University of Padova, Padova, Italy, in 2015. During his doctoral studies, he cooperated with several local companies for the design of permanent-magnet machines. In 2015, he joined the Power Electronics, Machines and Control Group, The University of Nottingham, Nottingham, U.K., as a Research Fellow, where he is currently an Assistant Professor teaching advanced courses on electrical machines. His main research interests include design and optimization of permanent-magnet machines, reluctance and permanent-magnet-assisted synchronous reluctance motors through genetic optimization techniques, for automotive and aerospace applications, ranging from small to large power.

Michael Galea (M'13) received his PhD in electrical machines design from the University of Nottingham, UK, where he has also worked as a Research Fellow. He is currently the Head of the School of Aerospace in the University of Nottingham, Ningbo, China, where he is also the Director of Aerospace. He is also the Deputy Director of the Institute for Aerospace Technology in the University of Nottingham, UK. He currently lectures in Electrical Drives and in Aerospace Systems Integration and manages a number of diverse projects and programmes related to the more / all electric aircraft, electrified propulsion and associated fields. His main research interests are design, analysis and thermal management of electrical machines and drives, the more electric aircraft and electrified and hybrid propulsion.

Chris Gerada (M'05–SM'12) received the Ph.D. degree in numerical modelling of electrical machines from The University of Nottingham, Nottingham, U.K., in 2005. He was a Researcher with The University of Nottingham, working on high-performance electrical drives and on the design and modelling of electromagnetic actuators for aerospace applications. Since 2006, he has been the Project Manager of the GE Aviation Strategic Partnership. In 2008, he became a Lecturer in electrical machines, in 2011, as an Associate Professor, and in 2013, a Professor at The University of Nottingham. His main research interests include the design and modelling of high-performance electric drives and machines. Prof. Gerada serves as an Associate Editor for the IEEE TRANSACTIONS ON INDUSTRY APPLICATIONS and is the Chair of the IEEE Industrial Electronics Society Electrical Machines Committee.